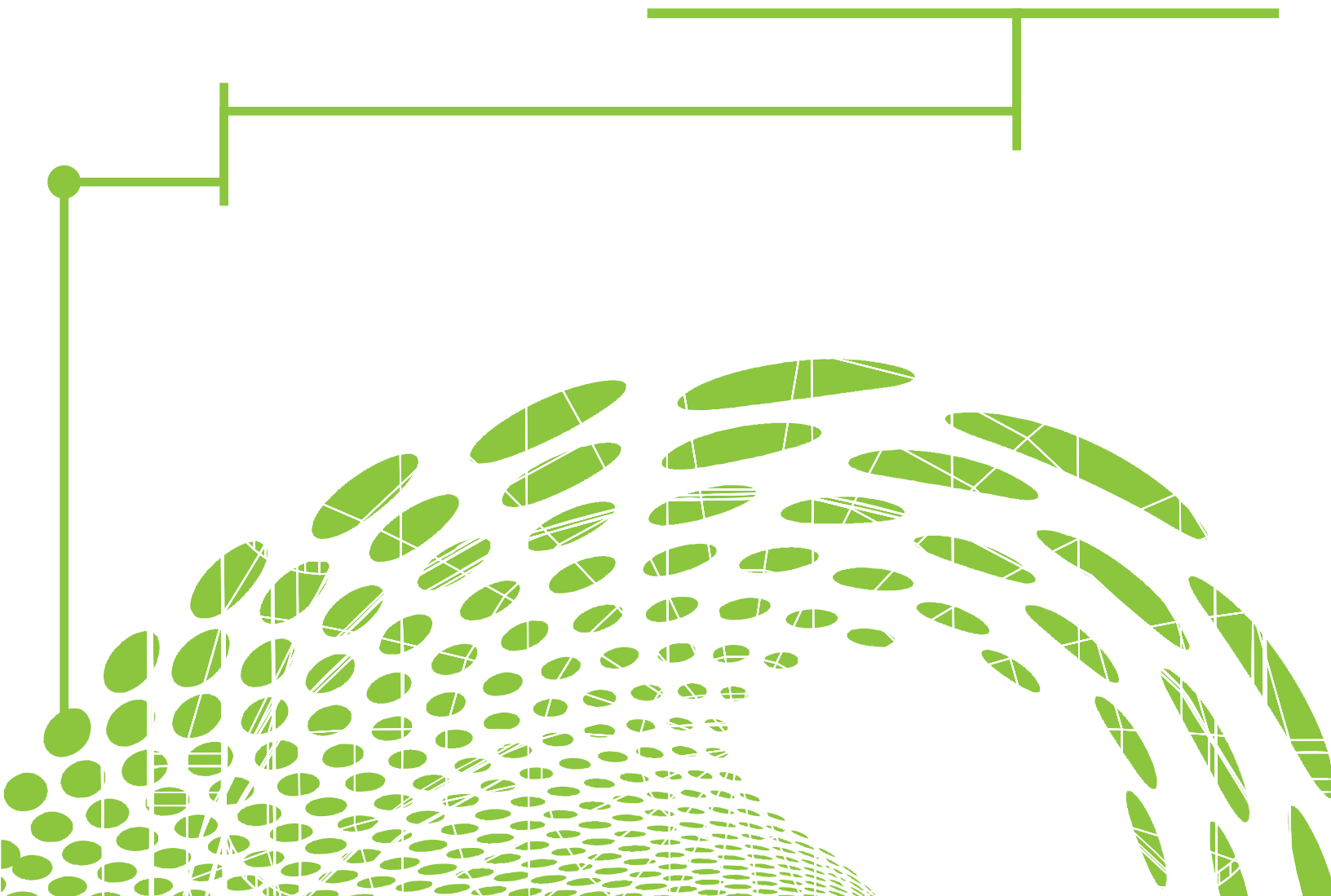




REFERENCE STRESS SOLUTIONS FOR THICK-WALL CYLINDERS



STP-PT-090

REFERENCE STRESS SOLUTIONS FOR THICK-WALL CYLINDERS

Prepared by:

Greg Thorwald, Ph.D., Principal Engineer
Lucie Parietti, Consulting Engineer
Quest Integrity USA, LLC



Date of Issuance: April 15, 2021

This publication was prepared by ASME Standards Technology, LLC (“ASME ST-LLC”) and sponsored by The American Society of Mechanical Engineers (“ASME”).

Neither ASME, ASME ST-LLC, the authors, nor others involved in the preparation or review of this publication, nor any of their respective employees, members, or persons acting on their behalf, makes any warranty, express or implied, or assumes any legal liability or responsibility for the accuracy, completeness, or usefulness of any information, apparatus, product or process disclosed, or represents that its use would not infringe upon privately owned rights.

Reference herein to any specific commercial product, process, or service by trade name, trademark, manufacturer, or otherwise does not necessarily constitute or imply its endorsement, recommendation, or favoring by ASME ST-LLC or others involved in the preparation or review of this publication, or any agency thereof. The views and opinions of the authors, contributors and reviewers of the publication expressed herein do not necessarily reflect those of ASME ST-LLC or others involved in the preparation or review of this publication, or any agency thereof.

ASME ST-LLC does not take any position with respect to the validity of any patent rights asserted in connection with any items mentioned in this document, and does not undertake to insure anyone utilizing a publication against liability for infringement of any applicable Letters Patent, nor assumes any such liability. Users of a publication are expressly advised that determination of the validity of any such patent rights, and the risk of infringement of such rights, is entirely their own responsibility.

Participation by federal agency representative(s) or person(s) affiliated with industry is not to be interpreted as government or industry endorsement of this publication.

ASME is the registered trademark of The American Society of Mechanical Engineers.

No part of this document may be reproduced in any form,
in an electronic retrieval system or otherwise,
without the prior written permission of the publisher.

ASME Standards Technology, LLC
Two Park Avenue, New York, NY 10016-5990

ISBN No. 978-0-7918-7450-9
Copyright © 2021
ASME Standards Technology, LLC
All Rights Reserved

TABLE OF CONTENTS

Foreword.....	x
Executive Summary.....	xi
1 Introduction.....	1
2 Scope of Work.....	3
3 Methodology.....	7
3.1 Reference Stress and Reference Stress Geometry Factor.....	7
3.2 Material Data Selection.....	10
3.2.1 Axial External Crack Model.....	12
3.2.2 Examine Geometry Factor Trend.....	14
3.2.3 Examine YS/TS Ratio for Additional Models.....	20
3.2.4 Material Choice for Project.....	23
3.3 Maximum Pressure Approach.....	24
3.3.1 Nominal Load and Geometry Factor Trends.....	34
3.3.2 J-Integral Trends.....	35
3.4 Reference Stress Comparison.....	37
3.5 Nominal Load Comparison to BPVC Collapse Pressure.....	41
4 Crack Cases.....	42
4.1 Axial Surface Cracks.....	42
4.1.1 Internal Axial Surface Cracks.....	42
4.1.2 External Axial Surface Cracks.....	44
4.2 Axial Full-Width Cracks.....	47
4.2.1 Internal Axial Full-Width Cracks.....	47
4.2.2 External Axial Full-Width Cracks.....	48
4.3 Circumferential Surface Cracks.....	50
4.3.1 Internal Circumferential Surface Cracks.....	50
4.3.2 External Circumferential Surface Cracks.....	52
4.4 Circumferential 360° Cracks.....	54
4.4.1 Internal Circumferential 360° Cracks.....	54
4.4.2 External Circumferential 360° Cracks.....	56
5 Results.....	59
5.1 Axial Surface Cracks.....	59
5.1.1 Internal Axial Surface Cracks.....	59
5.1.2 External Axial Surface Cracks.....	67
5.2 Axial Full-Width Cracks.....	74
5.2.1 Internal Axial Full-Width Cracks.....	74
5.2.2 External Axial Full-Width Cracks.....	77
5.3 Circumferential Surface Cracks.....	80
5.3.1 Internal Circumferential Surface Cracks.....	80
5.3.2 External Circumferential Surface Cracks.....	88
5.4 Circumferential 360° Cracks.....	95
5.4.1 Internal Circumferential 360° Cracks.....	95

5.4.2	External Circumferential 360° Cracks	98
6	Conclusions	102
6.1	Cases Examined	102
6.2	Methodology	102
6.3	Result Comparisons	102
6.4	Software Automation	103
6.5	Future Work	103
	References	104
	Appendix A: Nominal Load and Maximum Geometry Factor for Internal Axial Surface Cracks	105
	Appendix B: Nominal Load and Maximum Geometry Factor for External Axial Surface Cracks	111
	Appendix C: Nominal Load and Maximum Geometry Factor for Internal Axial Full-Width Surface Cracks	117
	Appendix D: Nominal Load and Maximum Geometry Factor for External Axial Full-Width Surface Cracks	119
	Appendix E: Nominal Load and Maximum Geometry Factor for Internal Circumferential Surface Cracks	121
	Appendix F: Nominal Load and Maximum Geometry Factor for External Circumferential Surface Cracks	127
	Appendix G: Nominal Load and Maximum Geometry Factor for Internal Circumferential 360° Surface Cracks	133
	Appendix H: Nominal Load and Maximum Geometry Factor for External Circumferential 360° Surface Cracks	135

LIST OF TABLES

Table 2-1:	Cylinder thickness Y ratios	3
Table 2-2:	Crack length a/l ratios	3
Table 2-3:	Crack depth a/T ratios	3
Table 2-4:	External circumferential crack length cases	4
Table 2-5:	Internal circumferential crack length cases	5
Table 2-6:	External cracks	6
Table 2-7:	Internal cracks	6

LIST OF FIGURES

Figure 1-1:	Failure Assessment Diagram example plot where the reference stress is used to determine the x-axis Lr assessment value.	1
Figure 3-1:	Infer the elastic J-integral trend from the first three results steps; the total J-integral value will begin increasing rapidly as plasticity develops at the crack front with increasing load; from Run ID 309 axial external full-width crack T/Ri = 2.0 and a/T = 0.2.	8
Figure 3-2:	The nominal load value is obtained at the intersection of the Kr ratio curve and the material specific value; from Run ID 309 axial external full-width crack T/Ri = 2.0 and a/T = 0.2. .9	
Figure 3-3:	Engineering stress-strain curves used to compare the YS/TS ratio on the reference stress results.	11

Figure 3-4: True stress-strain curves used with non-linear geometry to compare the YS/TS ratio on the reference stress results. 12

Figure 3-5: Cylinder with axial external surface crack: $R_i/T = 5$, $a/T = 0.4$; quarter symmetric model.13

Figure 3-6: Reference stress geometry factor results for YS/TS ratios and engineering versus true stress-strain curves; the axial external surface crack and cylinder dimensions are constant: $R_i/T = 5$, $a/T = 0.4$ 14

Figure 3-7: Von Mises stress results at the nominal load for YS/TS = 0.6, pressure = 8.96 ksi; color scale maximum set to YS = 60 ksi. 15

Figure 3-8: Von Mises stress results at the nominal load for YS/TS = 0.7, pressure = 11.96 ksi; color scale maximum set to YS = 70 ksi. 15

Figure 3-9: Crack front J-integral results along the surface crack at the nominal load; the crack tip is at left end of the plots and the crack depth location at the symmetry plane is at the right end of the plots. 16

Figure 3-10: Crack front reference stress results along the surface crack at the nominal load; the maximum crack front reference stress occurs near the crack tip, where the crack tip is at the left end of the plots and the crack depth location at the symmetry plane is at the right end of the plots. 17

Figure 3-11: J-integral versus pressure results at crack front node index 9 at the reference stress maximum value location along the surface crack front for YS/TS = 0.6 and 0.7 cases. 17

Figure 3-12: Kr ratio versus pressure trend intersection with the material specific ratio to obtain the nominal load for the two YS/TS ratios of 0.6 and 0.7. 18

Figure 3-13: Reference stress versus pressure load computed using the geometry factor F. 19

Figure 3-14: J-integral values for each contour around the crack front at the nominal load used to obtain the reference stress. 19

Figure 3-15: Geometry factor values versus the YS/TS ratio for several crack locations, orientations, and two cylinder R_i/T ratios; API 579 cylinder reference stress equation values are single points for comparison. 21

Figure 3-16: Lr values versus YS for external axis surface crack cases; compare Lr values computed using constant geometry factor F at YS/TS = 0.9 and Lr values computed using varying geometry factor F from YS/TS trends in Figure 3-15. 22

Figure 3-17: Normalized geometry factor values versus the YS/TS ratio for several crack locations, orientations, and two cylinder R_i/T ratios. 23

Figure 3-18: Engineering stress-strain curve used in this project to compute the reference stress for thick-wall cylinders; YS/TS = 0.9, YS = 90 ksi, TS = 100 ksi, modulus E = 30,000 ksi. ... 24

Figure 3-19: Crack mesh for Run 289 with 12 contours to compute the J-integral: $T/R_i = 2$, $a/T = 0.2$. 25

Figure 3-20: Von Mises stress results for Run 289 for increasing pressure showing the plastic zone extending through the cylinder thickness at higher pressure. 26

Figure 3-21: J-integral results versus pressure for Run 289; J_elastic is inferred from the first three load steps; J_average is the average of contours 2 through 12. 27

Figure 3-22: Kr ratio trend using J_contour_12 results for Run 289 to obtain the nominal load value at the intersection with the material specific Kr ratio; Kr ratio values above 1 are unusual behavior and may be due to the high stress on the thick-wall cylinder inside surface. 28

Figure 3-23: J-integral contour values for Run 289 for increasing pressure to the maximum converged pressure of 114 ksi; contour 1 are elements at the crack front; contour 12 are elements remote from the crack front. 29

Figure 3-24: J-integral results versus pressure for Run 293; the maximum converged pressure is 129 ksi.....30

Figure 3-25: Kr ratio versus pressure for Run 293; the maximum converged pressure is 129 ksi; the results were not sufficient to obtain the nominal load at the intersection of Kr and the material specific value.31

Figure 3-26: J-integral contour results for Run 293 for increasing pressure; the maximum converged pressure is 129 ksi.31

Figure 3-27: J-integral versus pressure results for Run 297 for increasing pressure; the maximum converged pressure is 142 ksi.32

Figure 3-28: Kr ratio versus pressure for Run 297; the maximum converged pressure is 142 ksi; an unusual trend of increasing Kr values.....33

Figure 3-29: J-integral contour results for Run 297 for increasing pressure; the maximum converged pressure is 142 ksi.33

Figure 3-30: Nominal pressure load versus crack depth ratio a/T for the full-width internal axial crack thick-wall cylinder T/Ri cases; the open orange circle data points near the grey arrow show the three a/T = 0.2 cases with unusual J-integral results behavior; extra data points at a/T = 0.25, 0.3, 0.35, and 0.38 were added to investigate the T/Ri = 3 cylinder.....34

Figure 3-31: Geometry factor results versus crack depth ratio a/T for the full-width internal axial crack thick-wall cylinder T/Ri cases; the open orange circle data points show the a/T cases with unusual J-integral results behavior; extra data points at a/T = 0.25, 0.3, 0.35, and 0.38 were added to investigate the T/Ri = 3 cylinder.35

Figure 3-32: J_{total}/J_{elastic} results versus pressure for the T/Ri = 1 cylinders; the J-integral results are sufficient to obtain the nominal load for all a/T crack depths.....36

Figure 3-33: J_{total}/J_{elastic} results versus pressure for the thickest T/Ri = 3 cylinders; the J-integral results are sufficient to obtain the nominal load for crack depths up to a/T = 0.3; the J-integral results are not sufficient for crack depths a/T = 0.2 and 0.25 to obtain the nominal load; the maximum converged pressure is used as an alternative nominal load for the shallow cracks.37

Figure 3-34: Hoop stress distribution through the cylinder thickness from outside to inside surface for T/Ri = 1 and pressure = 32,000 psi; the cylinder outside surface ‘OD’ is the left end of the plot.38

Figure 3-35: Reference stress versus crack length using the existing API 579 solution; compare the two linearized stress distributions; T/Ri = 1, a/T = 0.4.....39

Figure 3-36: Crack face pressure included in reference stress versus crack length using the existing API 579 solution; compare the two linearized stress distributions; T/Ri = 1, a/T = 0.4.40

Figure 3-37: Compare reference stress from J-integral method to existing API 579 solution; the API 579 solution uses the maximum linearized stress distribution; T/Ri = 1, a/T = 0.4.....40

Figure 3-38: Comparison of BPVC design pressure, FEA nominal load with a crack, and BPVC upper limit plastic collapse pressure for full-width internal axial shallow cracks a/T = 0.2.....41

Figure 3-39: Comparison of BPVC design pressure, FEA nominal load with a crack, and BPVC upper limit plastic collapse pressure for full-width internal circumferential shallow cracks a/T = 0.241

Figure 4-1: Quarter symmetric crack mesh case, Case 70, T/Ri = 2, a/c = 0.25, a/T = 0.6.42

Figure 4-2: Shallow crack mesh example, Case 33, T/Ri = 1.5, a/c = 0.0625, a/T = 0.2.43

Figure 4-3: Deep crack mesh example, Case 99, T/Ri = 2.5, a/c = 0.25, a/T = 0.6.44

Figure 4-4: Quarter symmetric crack mesh case, Case 211, T/Ri = 2, a/c = 0.25, a/T = 0.6.45

Figure 4-5: Shallow crack mesh example, Case 141, $T/R_i = 1$, $a/c = 0.03125$, $a/T = 0.2$46

Figure 4-6: Thickest cylinder example, Case 280, $T/R_i = 3$, $a/c = 2$, $a/T = 0.8$46

Figure 4-7: Internal full-width axial crack, Case 281, $T/R_i = 1$, $a/T = 0.2$47

Figure 4-8: Thickest cylinder, full-width internal axial crack, Case 300, $T/R_i = 3$, $a/T = 0.8$48

Figure 4-9: External full-width axial crack, Case 301, $T/R_i = 1$, $a/T = 0.2$49

Figure 4-10: Thickest cylinder, full-width external axial crack, Case 320, $T/R_i = 3$, $a/T = 0.8$50

Figure 4-11: Internal circumferential surface crack, Case 369, $T/R_i = 1$, $a/c = 0.125$, $a/T = 0.2$51

Figure 4-12: Internal circumferential surface crack, Case 468, $T/R_i = 2.5$, $a/c = 1$, $a/T = 0.8$51

Figure 4-13: External circumferential surface crack, Case 509, $T/R_i = 1$, $a/c = 0.125$, $a/T = 0.2$52

Figure 4-14: External circumferential surface crack, Case 538, $T/R_i = 1.5$, $a/c = 0.125$, $a/T = 0.4$53

Figure 4-15: External circumferential surface crack, Case 636, $T/R_i = 3$, $a/c = 1$, $a/T = 0.8$53

Figure 4-16: Internal circumferential 360° crack, Case 322, $T/R_i = 1$, $a/T = 0.4$54

Figure 4-17: 360° internal crack, Case 321, $T/R_i = 1$, $a/T = 0.2$, shallow crack example.55

Figure 4-18: 360° internal crack, Case 340, $T/R_i = 3$, $a/T = 0.8$, thickest cylinder.56

Figure 4-19: External circumferential 360° crack, Case 347, $T/R_i = 1.5$, $a/T = 0.6$57

Figure 4-20: 360° external crack, Case 341, $T/R_i = 1$, $a/T = 0.2$, shallow crack example.58

Figure 4-21: 360° external crack, Case 360, $T/R_i = 3$, $a/T = 0.8$, thickest cylinder.58

Figure 5-1: Nominal load plot for $T/R_i = 1$ for internal axial surface cracks.60

Figure 5-2: Nominal load plot for $T/R_i = 1.5$ for internal axial surface cracks.60

Figure 5-3: Nominal load plot for $T/R_i = 2$ for internal axial surface cracks.61

Figure 5-4: Nominal load plot for $T/R_i = 2.5$ for internal axial surface cracks.61

Figure 5-5: Nominal load plot for $T/R_i = 3$ for internal axial surface cracks.62

Figure 5-6: Maximum geometry factor for $T/R_i = 1$ for internal axial surface cracks.63

Figure 5-7: Maximum geometry factor for $T/R_i = 1.5$ for internal axial surface cracks.63

Figure 5-8: Maximum geometry factor for $T/R_i = 2$ for internal axial surface cracks.64

Figure 5-9: Maximum geometry factor for $T/R_i = 2.5$ for internal axial surface cracks.64

Figure 5-10: Maximum geometry factor for $T/R_i = 3$ for internal axial surface cracks.65

Figure 5-11: Von Mises stress contours for Case 33 ($T/R_i = 1.5$, $a/c = 0.0625$, $a/T = 0.2$) when slightly exceeding the nominal load. Stress scale is in ksi; deformation scale 5x for close-up crack mesh.66

Figure 5-12: Von Mises stress contours for Case 99 ($T/R_i = 2.5$, $a/c = 0.25$, $a/T = 0.6$) when slightly exceeding the nominal load. Stress scale is in ksi; deformation scale 5x for close-up crack mesh.66

Figure 5-13: Nominal load plot for $T/R_i = 1$ for external axial surface cracks.67

Figure 5-14: Nominal load plot for $T/R_i = 1.5$ for external axial surface cracks.68

Figure 5-15: Nominal load plot for $T/R_i = 2$ for external axial surface cracks.68

Figure 5-16: Nominal load plot for $T/R_i = 2.5$ for external axial surface cracks.69

Figure 5-17: Nominal load plot for $T/R_i = 3$ for external axial surface cracks.69

Figure 5-18: Maximum geometry factor plot for $T/R_i = 1$ for external axial surface cracks.70

Figure 5-19: Maximum geometry factor plot for $T/R_i = 1.5$ for external axial surface cracks.71

Figure 5-20: Maximum geometry factor plot for $T/R_i = 2$ for external axial surface cracks.71

Figure 5-21: Maximum geometry factor plot for $T/R_i = 2.5$ for external axial surface cracks.72

Figure 5-22: Maximum geometry factor plot for $T/R_i = 3$ for external axial surface cracks.72

Figure 5-23: Von Mises stress contours for Case 141 ($T/R_i = 1$, $a/c = 0.03125$, $a/T = 0.2$) when slightly exceeding the nominal load. Stress scale is in ksi; deformation scale 10x for close-up crack mesh.73

Figure 5-24: Von Mises stress contours for Case 280 ($T/R_i = 3$, $a/c = 0.2$, $a/T = 0.8$) when slightly exceeding the nominal load. Stress scale is in ksi; deformation scale 10x for close-up crack mesh.74

Figure 5-25: Nominal load plot for internal full-width axial surface cracks.75

Figure 5-26: Maximum geometry factor plot for internal full-width axial surface cracks.75

Figure 5-27: Von Mises stress contours for Case 281 ($T/R_i = 1$, $a/T = 0.2$) when slightly exceeding the nominal load. Stress scale is in ksi; deformation scale 1x for close-up crack mesh.76

Figure 5-28: Von Mises stress contours for Case 300 ($T/R_i = 3$, $a/T = 0.8$) when slightly exceeding the nominal load. Stress scale is in ksi; deformation scale 1x for close-up crack mesh.77

Figure 5-29: Nominal load plot for external full-width axial surface cracks.78

Figure 5-30: Maximum geometry factor plot for external full-width axial surface cracks.78

Figure 5-31: Von Mises stress contours for Case 301 ($T/R_i = 1$, $a/T = 0.2$) when slightly exceeding the nominal load. Stress scale is in ksi; deformation scale 10x for close-up crack mesh.79

Figure 5-32: Von Mises stress contours for Case 320 ($T/R_i = 3$, $a/T = 0.8$) when slightly exceeding the nominal load. Stress scale is in ksi; deformation scale 10x for close-up crack mesh.80

Figure 5-33: Nominal load plot for $T/R_i = 1$ for internal circumferential surface cracks.81

Figure 5-34: Nominal load plot for $T/R_i = 1.5$ for internal circumferential surface cracks.81

Figure 5-35: Nominal load plot for $T/R_i = 2$ for internal circumferential surface cracks.82

Figure 5-36: Nominal load plot for $T/R_i = 2.5$ for internal circumferential surface cracks.82

Figure 5-37: Nominal load plot for $T/R_i = 3$ for internal circumferential surface cracks.83

Figure 5-38: Maximum geometry factor plot for $T/R_i = 1$ for internal circumferential surface cracks.84

Figure 5-39: Maximum geometry factor plot for $T/R_i = 1.5$ for internal circumferential surface cracks.84

Figure 5-40: Maximum geometry factor plot for $T/R_i = 2$ for internal circumferential surface cracks.85

Figure 5-41: Maximum geometry factor plot for $T/R_i = 2.5$ for internal circumferential surface cracks.85

Figure 5-42: Maximum geometry factor plot for $T/R_i = 3$ for internal circumferential surface cracks.86

Figure 5-43: Von Mises stress contours for Case 369 ($T/R_i = 1$, $a/c = 0.125$, $a/T = 0.2$) when slightly exceeding the nominal load. Stress scale is in ksi; deformation scale 5x for close-up crack mesh.87

Figure 5-44: Von Mises stress contours for Case 468 ($T/R_i = 2.5$, $a/c = 1$, $a/T = 0.8$) when slightly exceeding the nominal load. Stress scale is in ksi; deformation scale 5x for close-up crack mesh.87

Figure 5-45: Nominal load plot for $T/R_i = 1$ for external circumferential surface cracks.88

Figure 5-46: Nominal load plot for $T/R_i = 1.5$ for external circumferential surface cracks.89

Figure 5-47: Nominal load plot for $T/R_i = 2$ for external circumferential surface cracks.89

Figure 5-48: Nominal load plot for $T/R_i = 2.5$ for external circumferential surface cracks.90

Figure 5-49: Nominal load plot for $T/R_i = 3$ for external circumferential surface cracks.90

Figure 5-50: Maximum geometry factor plot for $T/R_i = 1$ for external circumferential surface cracks.91

Figure 5-51: Maximum geometry factor plot for $T/R_i = 1.5$ for external circumferential surface cracks.92

Figure 5-52: Maximum geometry factor plot for $T/R_i = 2$ for external circumferential surface cracks.92

Figure 5-53: Maximum geometry factor plot for $T/R_i = 2.5$ for external circumferential surface cracks.93

Figure 5-54: Maximum geometry factor plot for $T/R_i = 3$ for external circumferential surface cracks.93

Figure 5-55: Von Mises stress contours for Case 538 ($T/R_i = 1.5$, $a/c = 0.125$, $a/T = 0.4$) when slightly exceeding the nominal load. Stress scale is in ksi; deformation scale 20x for close-up crack mesh.94

Figure 5-56: Von Mises stress contours for Case 636 ($T/R_i = 3$, $a/c = 1$, $a/T = 0.8$) when slightly exceeding the nominal load. Stress scale is in ksi; deformation scale 20x for close-up crack mesh.95

Figure 5-57: Nominal load plot for internal circumferential 360° surface cracks.....96

Figure 5-58: Maximum geometry factor plot for internal circumferential 360° surface cracks.96

Figure 5-59: Von Mises stress contours for Case 322 ($T/R_i = 1$, $a/T = 0.4$) when slightly exceeding the nominal load. Stress scale is in ksi; deformation scale 2x for close-up crack mesh.97

Figure 5-60: Von Mises stress contours for Case 340 ($T/R_i = 3$, $a/T = 0.8$) when slightly exceeding the nominal load. Stress scale is in ksi; deformation scale 10x for close-up crack mesh.98

Figure 5-61: Nominal load plot for external circumferential 360° surface cracks.....99

Figure 5-62: Nominal load plot for external circumferential 360° surface cracks.....99

Figure 5-63: Von Mises stress contours for Case 341 ($T/R_i = 1$, $a/T = 0.2$) when slightly exceeding the nominal load. Stress scale is in ksi; deformation scale 20x for close-up crack mesh.100

Figure 5-64: Von Mises stress contours for Case 360 ($T/R_i = 3$, $a/T = 0.8$) when slightly exceeding the nominal load. Stress scale is in ksi; deformation scale 10x for close-up crack mesh.101

FOREWORD

Acknowledgments

The authors gratefully acknowledge the ASME Peer Review Group members for their thoughtful review and guidance of this project. The ASME Peer Review Group members, in alphabetical order, are Anne Chaudouet, Ben Hantz, Mahendra Rana, Eric Roll, and J. Robert (Bob) Sims.

The authors also gratefully acknowledge the ASME Project Engineer Ray Rahaman and ASME ST-LLC Project Manager Dan Andrei for their help with organizing this project.

About ASME

Established in 1880, the ASME is a professional not-for-profit organization with more than 100,000 members and volunteers promoting the art, science and practice of mechanical and multidisciplinary engineering and allied sciences. ASME develops codes and standards that enhance public safety, and provides lifelong learning and technical exchange opportunities benefiting the engineering and technology community. Visit <https://www.asme.org/> for more information.

ASME ST-LLC is a not-for-profit Limited Liability Company, with ASME as the sole member, formed in 2004 to carry out work related to new and developing technology. ASME ST-LLC's mission includes meeting the needs of industry and government by providing new standards-related products and services, which advance the application of emerging and newly commercialized science and technology, and providing the research and technology development needed to establish and maintain the technical relevance of codes and standards. Visit <http://asmestllc.org/> for more information.

EXECUTIVE SUMMARY

This report describes the analysis completed to obtain crack front maximum reference stress results for internal and external cracks in thick-walled cylinders. The crack models and analysis method compute the geometry factor that is used to compute the reference stress value for a given assessment pressure. The reference stress is needed to obtain the Lr ratio for the Failure Assessment Diagram (FAD) method to assess cracks for stability, which is described in Section 1. The geometry factor results are tabulated in the appendices of this report and in the Excel file attached to this report.

Three dimensional surface plots of nominal load and maximum geometry factor results are given for each crack case to show the results trend versus the cylinder geometry ratios. The results are reported as non-dimensional geometry factors that are tabulated in the report appendices for all cases. For use in crack assessments, the geometry factors would be used with a table look-up. For geometry and crack dimensions with intermediate ratios between the table values, interpolation would be used to obtain the geometry factor.

Cases Examined

The 523 thick-wall cylinder cases examined in this project include a range of geometry ratios for the cylinder thickness to radius ratio, crack depth to thickness ratio, crack length to crack depth ratio for the surface cracks, and four crack locations: axial internal, axial external, circumferential internal, and circumferential external. The crack shapes include surface cracks, axial full-width partial depth axial cracks, and circumferential 360° partial-depth cracks. The full-width and 360° crack shapes provide bounding solutions for the longest surface crack results so that the solutions presented here can be applied to longer surface cracks.

Methodology

Elastic-plastic Finite Element Analysis (FEA) was used to compute the crack front J-integral results versus increasing internal pressure. The J-integral results are used to obtain the nominal load using the Kr ratio intersection with the material-specific ratio, which is a function of the material's yield strength and elastic modulus. Using the nominal load, the geometry factor values were computed. The geometry factors are used to compute the reference stress and FAD Lr ratio. The J-integral nominal load methodology is described in Section 3.1 of this report. The stress-strain curve used for this project was initially examined using a range of yield strength to tensile strength ratios. The investigation revealed a dependency of the reference stress on the yield to tensile strength ratio. The investigation results led to the choice of a stress-strain curve with a yield to tensile strength ratio of 0.9, which is described in Section 3.2.

As the cylinder thickness increases, some shallow internal cracks had insufficient J-integral results to obtain the nominal load; the Kr ratio did not intersect with the material specific ratio. An alternative method of using the maximum converged pressure was used to obtain a nominal load so that the geometry factor could be computed for all the cases in this project. Section 3.3 discusses the maximum pressure approach and compares trends to the J-integral method.

Result Comparisons

The thick-wall cylinder reference stress results from this project were compared to the existing reference stress solution from API 579 in Section 3.4. The comparison shows similar reference stress result values for the radius to thickness ratio of 1.0, the thinnest cylinder geometry in this project. Since the thick-wall

cylinder hoop stress has a curved non-linear distribution through the thickness, and the current API 579 reference stress solution is in terms of a linear membrane plus bending stress, the thick-wall cylinder reference stress solutions better capture the actual hoop stress and thick-wall geometry to give an improved reference stress result to evaluate cracks in thick-wall cylinders.

Another result comparison was with the maximum collapse pressure of undamaged cylinders using the ASME Boiler Pressure Vessel Code Section VIII Division 3 pressure design equations. The cracked cylinder nominal load was less than the maximum collapse pressure of an undamaged cylinder, indicating the results capture the reduced maximum pressure of a cracked cylinder.

Software Automation

The crack meshes were created using Quest Integrity's FEACrack software, and the analyses were run using the Abaqus FEA software. Python scripts were used to update the geometry data and generate all 523 models by running the FEACrack software automatically, which removes human error from the crack mesh generation. The FEA results files were post-processed using FEACrack to extract the stress, deformation, and crack front J-integral results. The FEACrack post-processing module automatically computes the nominal load, geometry factor, and reference stress along the crack front and reports the maximum crack front reference stress results. A second Python script extracted these maximum crack front reference results from the output report text files to tabulate and plot the results for each model group.

Future Work

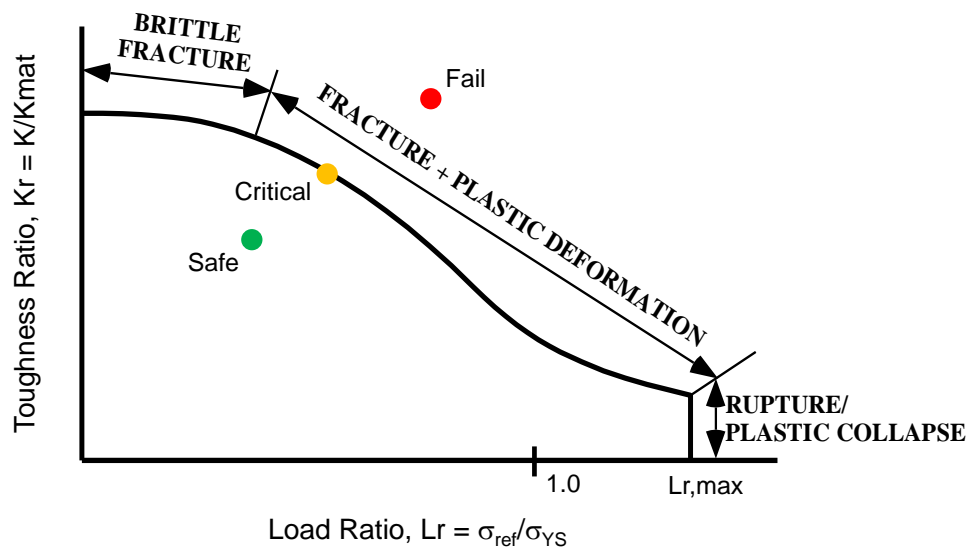
The tabular reference stress results can be reviewed and added to appropriate ASME standards, such as the API 579/ASME FFS-1 standard, to aid in evaluating cracked thick-wall cylinder components for high pressure applications. Since the reference stress was shown to have a dependence on the material yield strength to tensile strength ratio, some additional cases could be examined to determine if the trends in this report continue for thicker cylinder cases. A scalar multiplier as a function of the yield to tensile strength ratio could be developed that would be used to multiply the reference stress geometry factor solutions in this report, which were developed using a yield to tensile strength ratio of 0.9, to extend use of these solutions to smaller yield to tensile strength ratios.

To obtain a better overlap of the thick-wall cylinder reference stress solutions with the current reference stress solution in API 579, some thinner wall cylinder cases could be examined where the hoop stress distribution through the thickness is linear, which would match the stress distribution used in the current solution.

1 INTRODUCTION

Evaluating cylinders with cracks using the Failure Assessment Diagram (FAD) fracture mechanics methodology requires a reference stress solution to check for plastic collapse. An example FAD plot is shown in Figure 1-1. The L_r value on the FAD x-axis is the ratio of the reference stress to the yield strength. The K_r value on the FAD y-axis is the ratio of the crack front stress intensity to the toughness. To assess a cracked cylinder, the L_r, K_r point is computed using the cylinder dimensions, crack dimensions and orientation, and the applied loading. Assessment points below the FAD curve indicate a stable crack and are considered safe, where points outside the FAD curve predict an unstable crack that would cause a failure of the cylinder. An assessment point on the FAD curve is at the critical limit, and can be used to determine a critical crack size or a critical load, such as burst pressure. The shape of the FAD curve captures the interaction of the two material failure modes: brittle fracture and plastic collapse.

Figure 1-1: Failure Assessment Diagram example plot where the reference stress is used to determine the x-axis L_r assessment value.



The API 579/ASME FFS-1 2016 standard [1] provides reference stress solutions for cylinders with cracks for a limited range of diameter to thickness ratios for thinner wall cylinders. Reference stress solutions for thick-walled cylinders are not yet available in API 579, so additional solutions are needed to support thick-wall cylinder cases. Adding reference stress solutions for thick-walled cylinders would be beneficial to evaluate cracks in high pressure thick-wall vessels and piping.

Reference stress solutions can be determined using elastic-plastic Finite Element Analysis (FEA) of cracked cylinders. The crack front J-integral is computed for a range of increasing pressure values. The J-integral results are used to determine a nominal load and geometry factor that gives the reference stress using the methodology in API 579; refer to Section 3.1 in this report for more details. The non-dimensional geometry factor values are obtained for a range of cylinder and crack geometries and are tabulated in the appendices at the end of this report.

Two previous Standards Technology Publications [2][3] provided stress intensity K solutions for thick-walled cylinders. Stress intensity solutions are used to obtain the K_r value on the FAD y-axis. However,